Acta Pharmacologica Sinica (2009) 30: 1577–1584

www.nature.com/aps

Original Article

Drug packaging and delivery using perfluorocarbon nanoparticles for targeted inhibition of vascular smooth muscle cells

Zhao-xiong ZHOU[1], Bai-gen ZHANG[1], Hao ZHANG[1], Xiao-zhong HUANG[1], Ya-li HU[1], Li SUN[2], Xiao-min WANG[2], Ji-wei ZHANG[1,*]

[1]*Department of Vascular Surgery, Shanghai Renji Hospital, Affiliated with the Shanghai Jiaotong University School of Medicine;*
[2]*Department of Pharmacy, Shanghai 200001, China*

Aim: To investigate the *in vitro* release profile of drugs encapsulated within perfluorocarbon (PFC) nanoparticles (NPs) and their ability to inhibit the activity of vascular smooth muscle cells (SMCs).
Methods: Dexamethasone phosphate (DxP) or dexamethasone acetate (DxA) was encapsulated into PFC nanoparticles using a high-pressure homogenous method. The morphology and size of the NPs were examined using scanning electron microscopy (SEM) and a laser particle size analyzer. Drug loading and *in vitro* release were assessed by high-performance liquid chromatography (HPLC). The impact of NP capsules on SMC proliferation, migration and apoptosis *in vitro* was assessed using cell counting kit-8, transwell cell migration and flow cytometry assays.
Results: The sizes of DxP-NPs and DxA-NPs were 224±6 nm and 236±9 nm, respectively. The encapsulation efficiency (EE) of DxP-NPs was 66.4%±1.0%, with an initial release rate of 77.2%, whereas the EE of DxA-NPs was 95.3%±1.3%, with an initial release rate of 23.6%. Both of the NP-coated drugs could be released over 7 d. Human umbilical artery SMCs were harvested and cultured for four to six passages. Compared to free DxP, SMCs treated with tissue factor (TF)-directed DxP-NPs showed significant differences in the inhibition of proliferation, migration and apoptosis ($P<0.05$).
Conclusion: The results collectively suggest that PFC nanoparticles will be beneficial for targeted drug delivery because of the sustained drug release and effective inhibition of SMC proliferation and migration.

Keywords: fluorocarbons; nanoparticles; restenosis; smooth muscle cells; sustained release

Acta Pharmacologica Sinica (2009) 30: 1577–1584; doi: 10.1038/aps.2009.146

Introduction

Restenosis remains the major limitation of percutaneous transluminal angioplasty and stenting in the treatment of patients with atherosclerotic disease[1, 2]. Although a number of factors are involved in the pathogenesis of vascular restructuring, the defining feature of restenosis is the proliferation and migration of smooth muscle cells (SMCs) from the media to the intima[3, 4]. Recently, drug-eluting stents were successfully introduced in interventional procedures and led to an accentuated drop in the restenosis rate[5, 6]. Many new antiproliferative compounds are currently under evaluation to be loaded onto stents, including dexamethasone[7]. However, the extensive drug distribution and burst release of the drug within the coated polymer could result in thrombosis, aneurysm formation, and an inflammatory reaction limited to the arterial wall surrounding the stent[8, 9].

With the use of nanotechnology, it is becoming possible to target drug molecules to the site of action, paving the way for personalized medicine that reduces the effect of the drug on other sites while maximizing its therapeutic effect. Liposomes, emulsions and polymer-based nanoparticles are the most widely used drug delivery systems, as these compounds are generally biodegradable, do not accumulate in the body and are possibly risk-free[10].

Perfluorocarbon (PFC) nanoparticles are novel paramagnetic contrast agents used in contrast agent design and drug delivery[11]. PFC has a structure similar to that of hydrocarbons, except that all the hydrogen atoms are replaced with fluorine. As there is no fluorine in the human body naturally, PFC can be introduced into the blood as a contrast agent for magnetic resonance (MR) imaging. PFC nanoparticles are stabilized for *in vivo* use with surfactants; the most common surfactants

* To whom correspondence should be addressed.
E-mail zhangjiwei001@sina.com
Received 2009-03-25 Accepted 2009-08-27

are phospholipids, which restrict the ability of the PFC cores to coalesce with one another. The phospholipid surface can also provide an ideal location for the incorporation of specialized components, such as targeting ligands and therapeutic drugs[12].

In this study, Dexamethasone Phosphate (DxP) and Dexamethasone Acetate (DxA) were tested as candidates for a therapeutic drug model encapsulated by nanoparticles. The difference in solubility between the two drugs was compared by an *in vitro* dissolution assay. Moreover, SMCs were treated with free DxP and tissue factor (TF)-targeted NPs loaded with DxP *in vitro*, which allowed for evaluating the feasibility of the nanoparticle drug delivery system for the targeted inhibition of SMC proliferation.

Materials and methods

Materials

Dexamethasone Phosphate (DxP) and Dexamethasone Acetate (DxA) were purchased from Shanghai Tongyong Pharmaceutical Co (China). The reference profiles of DxP and DxA were obtained from the National Institute of Control of Pharmaceutical Biological Products (NICPBP, China). Perfluorooctylbromide (boiling point 142 °C) was purchased from Gateway Specialty Chemicals (USA). Biotinylated phosphatidylethanolamine (PE) and biotinylated rabbit anti-human Tissue Factor (TF) antibodies were supplied by Sino-American Biotechnique Co (China). Lecithin, cholesterol and safflower oil were all purchased from Sigma (USA). Cellulose membranes (Membra-cell, with a molecular weight cut-off of 14 000) were supplied by Polylab (France).

Nanoparticle preparation

The biotinylated PFC nanoparticles were produced by incorporating DxP or DxA into the outer lipid layer of a PFC microemulsion, using a high-pressure homogeneous method[12]. Briefly, the emulsion comprised 20% *v/v* perfluorooctylbromide and 2% *w/v* lipid mixture. The lipid mixture included 60% *w/w* lecithin (containing 20 mg biotinylated PE), 30% *w/w* cholesterol and 10% *w/w* DxP or DxA, which were all dissolved in chloroform, evaporated under reduced pressure, dried in a 35 °C vacuum oven and dispersed in water using an ultrasonicator (Sonics vibracell, USA). The suspension was combined with 20% *v/v* perfluorooctylbromide, 2% *v/v* safflower oil and distilled deionized water, and it was processed continuously at 0.7 kPa for three cycles and 1.5 kPa for three cycles, using a high-pressure homogenizer (Niro Soavi NS1001L, Italy).

Morphology of drug-loaded NPs

The morphology of the nanoparticles was characterized by scanning electron microscopy (SEM XL40, Philips). The nanoparticle samples were prepared by putting a drop of the particle dispersion on a cleaned glass cover slide, which was then dried for 2 h at room temperature. The slides were mounted on aluminum pins using double-sided adhesive tape. Prior to SEM examination, the samples were coated with a gold layer under vacuum for 30 s.

Particle size and zeta potential analysis

Particle size was determined using a laser light-scattering submicron particle size analyzer (NICOMP 380ZLS, USA). A dilute suspension of nanoparticles (1:20) was prepared in doubly distilled water and sonicated in an ice bath for 30 s. The sample was subjected to particle size and zeta potential analysis, which was conducted in triplicate at 37 °C.

Encapsulation efficiency (EE)

Samples (100 μL) of NPs were taken in triplicate and dissolved in 900 mL of methanol, after which the total amount of drug delivered by the NPs was quantified by HPLC[13]. The amount of non-entrapped drug recovered in the supernatant was measured after ultracentrifugation of the NPs at 64 000×*g* for 1 h. Encapsulation efficiency was calculated by the following formula: EE%=[1–(unencapsulated drug/total drug)]×100%.

HPLC analysis of DxP and DxA

The HPLC system used to analyze DxP and DxA included a Waters 2487 ultraviolet detector (wavelength 240 nm), a Waters 1525 sample processor and a Diamonsil C18 column (4.6×250 mm, 5 μm). A mixture of methanol and water (74:26, *v/v*) was employed as the mobile phase for DxA detection, at a flow rate of 1 mL/min. The mobile phase for DxP was 0.05 mol/L PBS/acetonitrile/acetic acid in a 70:28:2 ratio, flowing at 1 mL/min at ambient temperature.

In vitro drug release from NPs

The *in vitro* release of the drugs from nanoparticles was assessed under sink conditions using side-by-side double-diffusion chambers, separated by a dialysis membrane (MEMBRAE-CELL, France) with a molecular weight cut-off of 14 000 Dalton. A 5-mL suspension of drug-loaded nanoparticles was placed in the donor chamber, and the receiver chamber[12] contained 200 mL of 0.9% saline supplemented with 0.2 mg/mL human serum albumin (Shanghai RAAS, China). The chambers were then placed in an orbital shaker (THC-D orbital shaker, Taicang Lab Instrument, China) maintained at 37 °C and 60 r/min. At appropriate intervals, 200-μL aliquots of the receiver medium were withdrawn and immediately replaced with an equal volume of fresh buffer. Free drug concentrations within the receiver media were analyzed in duplicate with high-pressure liquid chromatography, as described above.

SMC culture

SMCs were cultured from human umbilical artery blood, using the explant technique[14]. Umbilical cord samples were obtained from healthy pregnant women after a normal delivery. The research was carried out according to the principles of the Declaration of Helsinki and was approved by the board of ethics committee of Shanghai Renji Hospital. The artery from the umbilicus was isolated surgically, and the tissue was minced into small pieces. The pieces were plated onto a

fibronectin-coated Petri dish and cultured in DMEM medium (Gibco) with 10% heat-inactivated FCS (Gibco), 2 mmol/L glutamine (Gibco), 100 U/mL penicillin and 100 μg/mL streptomycin in a humidified atmosphere of 5% CO_2 and 95% air. Cells were subcultured with 0.125% trypsin-EDTA (Gibco) when there was adequate proliferation beyond the explants. SMCs were characterized by immunohistochemical staining for smooth muscle-specific α-actin. Further studies were performed on cells at passages 4 through 6 and 80%–90% confluence.

SMC proliferation assay

For the proliferation assay, cells were plated at a concentration of 10 000 cells in 0.1 mL of 10% FBS-DMEM per well, in 96-well plates. After 24 h of incubation, cells were serum-starved for 48 h and treated as below.

To evaluate the dose effects of DxP on SMC proliferation, the wells were replenished with serum-free media with different concentrations of DxP (1, 5, 10, 100 μg/mL) and cultured for 3 or 6 d. To assess the proliferative activity of SMCs, the number of cells was measured using Cell Counting Kit-8 (CCK-8), according to the manufacturer's recommendations (Dojindo, Kumamoto, Japan)[15]. Briefly, 10 μL of CCK-8 was added to each well and incubated at 37 °C for an additional 2 h. Absorbance at 450 nm was measured using the BioRad 680 microplate reader (USA). The results of the CCK-8 assay are nearly proportional to the cell number and can thus be used to determine proliferation and cytotoxicity.

To investigate the ability of SMCs inhibited by targeted NPs, SMCs (n=5 per treatment) were exposed sequentially to excess biotinylated anti-TF antibody, avidin (Amresco, USA) and then biotinylated DxP nanoparticles. Positive control groups were exposed to 10 μg/mL DxP (equivalent to theoretical drug loading) and 1% *v/v* PFC (PFC content equivalent to NPs) in buffer. Unbound nanoparticles and unabsorbed drug were washed from wells. After treatment, SMCs were cultured in normal conditions for 3 d. The number of attached viable cells was counted as described above.

SMCs were also grown on glass coverslips and treated with TF-targeted DxP-NP or 10 μg/mL DxP for 18 h and then stained using routine Hematoxylin and Eosin methods or smooth muscle-specific α-actin immunofluorescence for morphological observation.

SMC migration

Cell migration was measured using the Transwell cell migration assay[16]. Briefly, human umbilical artery SMCs were suspended at a concentration of 2×10^5 cells/mL after overnight serum starvation. Aliquots of 0.1 mL of cells (2×10^4 cells) were added to the upper chamber (fibronectin-coated, 8-μm pore size, Costar) and allowed to attach for 2 h. The upper chambers were then transferred to the lower transwell compartment with conditioned media containing 0.6 mL of 0.5% FCS/DMEM, migration factors such as PDGF-BB (5 ng/mL, PeproTech) and VEGF (10 ng/mL, Pepro Tech); TF-targeted DxP-NPs (5% *v/v*) or DxP (10 μg/mL) were also added. After incubation at 37 °C in 5% CO_2 for 6 h, cells remaining on the upper membrane surface were removed mechanically with a cotton swab. Cells that had migrated to the lower side of the membrane were fixed and stained with toluidine blue. The number of cells was counted in five separate high-power fields at a magnification of 200× (Nikon). The experiments described were repeated a minimum of three times, and SMC migration was averaged and expressed as mean±SD.

Analysis of apoptosis by flow cytometry

Annexin V binding and propidium iodide staining were carried out using the Annexin V-FITC Apoptosis Detection Kit I (BD Pharmingen) and flow cytometry[17]. Briefly, human umbilical artery SMCs (passage four to six, 80%–90% confluence) were exposed to TF-targeted DxP-NPs (5% *v/v*) or 10 μg/mL DxP in 0.5% FCS/DMEM media for 4 h, then washed twice and resuspended at a concentration of 1×10^6 cells/mL; 100 μL of cells was mixed with 5 μL each of Annexin V-FITC and propidium iodide for 15 min at room temperature in the dark. After adding 400 μL of binding buffer, cells were analyzed by flow cytometry (FACSCalibur, BD Biosciences). The percentage of cells undergoing apoptosis was determined according to the manufacturer's instructions for the apoptosis detection kit.

Statistical analysis

Data are expressed as means±SD. Statistical analysis of differences between different treatments was assessed with Student's t test or ANOVA, as appropriate. A 0.05 level of probability was used as the threshold for significance.

Results

Characterization of drug-loaded PFC NPs

The SEM morphological observation of NPs loaded with DxP or DxA demonstrated uniform, rounded particles. Based on the smooth spherical surface of NPs, no drug nanocrystals had formed around the NPs (Figure 1). The particle sizes of both DxP and DxA presented a normal distribution, with the chi-squared values being 1.95 and 0.79, respectively. The particle sizes, zeta potentials and encapsulation efficiencies are shown in Table 1. The average diameter of drug-loaded NPs was comparable (P>0.05) to that of the NPs without drugs. As

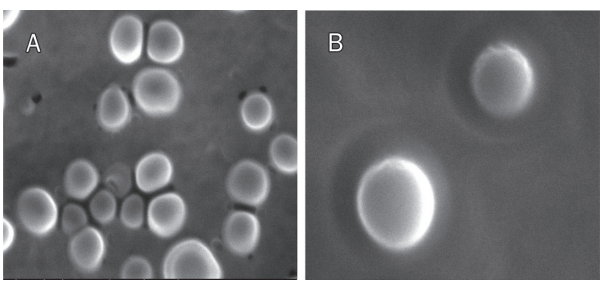

Figure 1. Morphological appearance of drug-loaded nanoparticles under scanning electron microscopy. (A) DxP-loaded PFC nanoparticles (×10 000), (B) DxA-loaded PFC nanoparticles (×28000).

Table 1. Characterization of PFC nanoparticles and drug-loaded PFC nanoparticles by mean diameter, zeta potential and encapsulation efficiency (EE). Each value represents the mean±SD. n= 3.

Code	Mean diameter (nm)	Zeta potential (mV)	EE (%)
NPs[a]	221±3.7	32±1.4	
DxP-NPs[b]	224±6.2	18±1.7	66.4±1.0
DxA-NPs[c]	236±9.3	43±2.3	95.3±1.3

[a]NPs, perfluorocarbon nanoparticles
[b]DxP-NP, dexamethasone phosphate-loaded perfluorocarbon nanoparticles
[c]DxA-NP, dexamethasone acetate-loaded perfluorocarbon nanoparticles

depicted in Table 1, there were significant differences (P<0.05) in zeta potential and EE between DxP-NPs and DxA-NPs.

In vitro drug release from NPs

The release of DxP and DxA from PFC nanoparticles *in vitro* is depicted in Figure 2. The early release phase is dominated by an initial drug burst. In the case of DxP-NPs, 77.2%±2.6% of the encapsulated DxP was released during the first day. DxA-NPs exhibited a lower burst release of approximately 23.6%±1.7% in the first day. The following release phase for both NPs was characterized by a slow but continuous profile over a time period of 7 days.

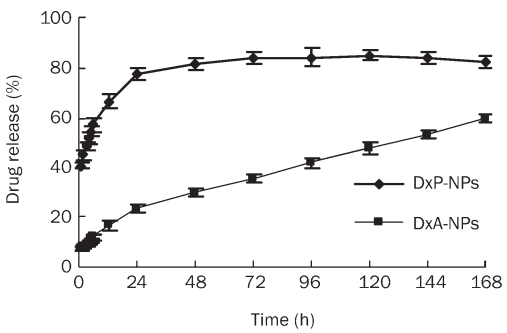

Figure 2. *In vitro* release of dexamethasone phosphate (DxP) and dexamethasone acetate (DxA) from perfluorocarbon nanoparticles (NPs). The amount of drug released from the nanospheres was quantified by HPLC. Data are means±SD. (n=3).

Effect of DxP on SMC proliferation

As shown in Figure 3, normal human umbilical artery SMCs in primary culture exhibited a typical phenotype with a characteristic spindle-shaped morphology and the presence of actin stress fibers. At confluence, spontaneous retraction occurs and produces a "hill and valley" pattern. Cell proliferation assays were performed on SMCs at passages 4 to 6. Control cells that had been incubated with normal growth medium continued to grow until they reached confluence. In contrast, cells incubated with DxP-containing medium were attenuated in a concentration-dependent manner for 3 or 6 d (Figure 4).

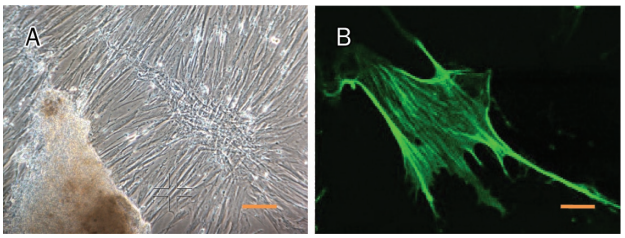

Figure 3. Morphology of normal SMC. (A) Phase contrast micrograph of human umbilical vascular smooth muscle cell (SMC) showing the hill and valley morphology, scale bar 200 μm. (B) Fluorescence micrograph of SMCs stained with mouse anti-human SMC α-actin, scale bar 20 μm.

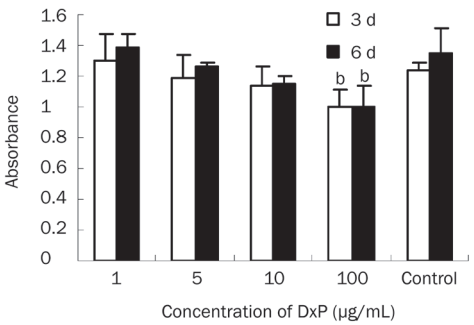

Figure 4. Effect of dexamethasone phosphate (DxP) on SMC proliferation. The number of cells was determined with a CCK-8 kit after 3 or 6 d of exposure to DxP. The absorbance value (at 450 nm) is proportional to the number of living cells. Data are represented as means±SD. DxP inhibited the proliferation of SMCs in a concentration-dependent manner. [b]P<0.05 compared to control.

Compared to the control, the number of cells was significantly lower in the group treated with 100 μg/mL DxP (P<0.05). No additional drug was added in the 6-day group, and prolongation of treatment did not result in any further inhibition of SMC proliferation.

Therapy targeting the proliferation of SMCs

Three days after the 30-min exposure, the anti-proliferative effects of the TF-targeted DxP-NPs and control PFC or free DxP were quantified (Table 2). TF-targeted DxP-NPs markedly decreased cell number by almost 40% compared to the control, and they resulted in dramatic morphological changes, such as condensed nuclei and a disrupted α-actin cytoskeleton

Table 2. Effect of DxP-NPs, DxP and PFC on the proliferation of SMCs. n=5. [b]P<0.05 vs control; [e]P<0.05 *vs* DxP or PFC.

	Group			
	Control	DxP-NPs[1]	DxP	PFC
Mean±SD	1.279±0.023	0.782±0.069[be]	1.105±0.036	1.208±0.03
RGR*	1	0.61	0.863	0.944

*RGR, relative growth rate

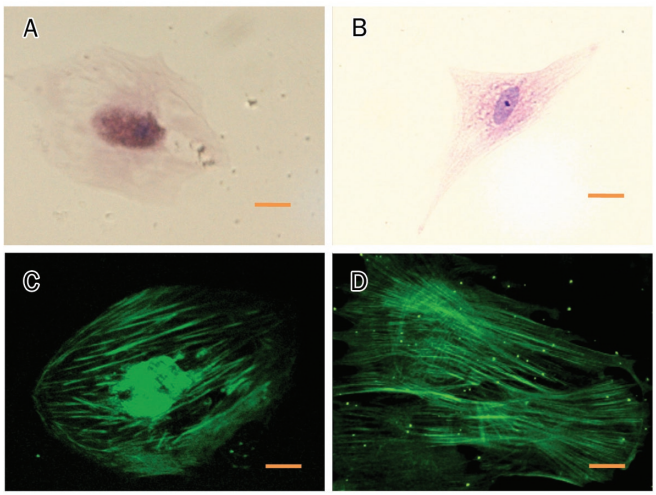

Figure 5. Smooth muscle α-actin of SMCs exposed to TF-targeted DxP-NPs (5% *v/v*) (A, C) and exposed to 10 μg/mL DxP (B, D) Routine HE and immunofluorescence staining were used in the upper and lower pannels, respectively. Scale bar 20 μm.

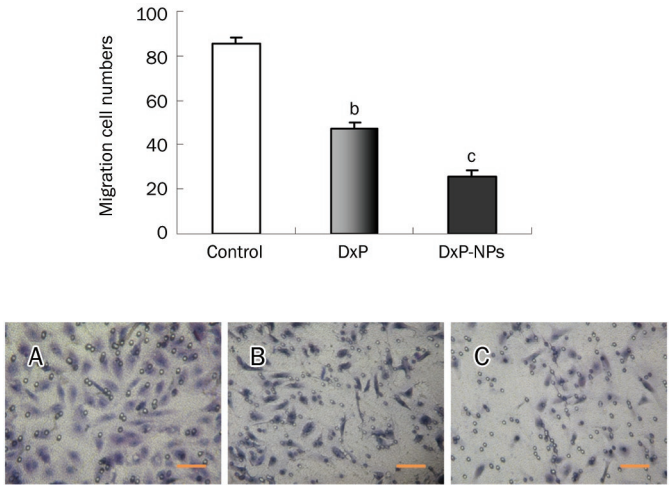

Figure 6. Effect of DxP-NPs or DxP on SMC migration. (Top) Migration assay was performed 6 h after the addition of DxP-NPs or free DxP to the lower chamber. For each experiment, five random fields were counted. Values are expressed as means±SD (n=4). ^{b}P<0.05, ^{c}P<0.01 compared to the control, respectively. (Bottom) Representative views of migrated cells (blue, spindle-like) from each sample. A, control. B, treated with free DxP. C, treated with TF-targeted DxP-NPs; scale bar 100 μm.

in many surviving cells (Figures 5A and 5C). However, free DxP mildly inhibited cell proliferation and produced no obvious morphological changes (Figures 5B and 5D). PFC, the core of the nanoparticle, had no obvious toxicity on the proliferation of SMCs (P>0.05 *vs* control).

SMC migration assay

The transwell cell migration assay was performed to compare the effect of TF-targeted DxP and free DxP on growth factor-induced SMC migration. Human umbilical artery SMCs induced by PDGF and VEGF showed relatively high migration activity (85.7±3.0). This response was inhibited by DxP (47.3±2.6, P<0.05). Compared to the DxP group, TF-targeted DxP-NPs exhibited an enhanced inhibition effect on SMC migration (25.8±2.5, P<0.05, Figure 6).

SMC apoptosis assay

Apoptosis in human umbilical artery SMCs was measured after treatment of the cells for 4 h with free DxP or TF-targeted DxP-NPs. To confirm that the loss in cell viability was due to apoptosis, we used FITC-conjugated Annexin V and Propium Iodide (PI). Annexin V staining can identify apoptosis at an earlier stage based on nuclear changes. The results in Figure 7 show quantitative apoptotic activity induced by free DxP and TF-targeted DxP-NPs. Early apoptotic (Annexin V+/PI–), late apoptotic (Annexin V+/PI+) and damaged (AnnexinV–/PI+) cells were distinguished on the basis of double-labeling for Annexin V-FITC and PI. The scatter plots show that there was no significant difference in the amount of apoptotic cells treated by free drug DxP or TF-targeted DxP-NPs (76.7±8.7 *vs* 76.5±15.4, P>0.05), but there were significant difference in late cellular apoptosis when SMCs were induced by TF-targeted DxP-NPs (6.4±2.8) compared to treatment with free DxP (1.6±0.4, P<0.05).

Discussion

Drug-loaded PFC nanoparticles were produced using a high-pressure homogenous method. In this study, Dexamethasone Phosphate (DxP) or Dexamethasone Acetate (DxA) was dissolved in an organic solvent. Phospholipids, which acted as surfactants, were also dissolved in the solvent, restricting the ability of the PFC cores to coalesce with one another[18]. The phospholipid surface also provides an ideal location for the incorporation of targeting ligands. After further processing of the solution using an ultrasonicator, drugs were fully diffused into the lipid layer, and the solvent was removed from the fine emulsion[12]. Then, the high-pressure homogenizer was used to achieve a further reduction in particle size, yielding a round uniform profile with a normal Gaussian distribution.

The ratio of drug to phospholipids was maintained at 1:9 to achieve a good dispersion of the drug in the lipid layer. The process of phase separation/coacervation has been well established[19]. The ratio of PFC/safflower oil/phospholipids was 10:1:1. These ratios are within the "stability window" for optimal encapusulation of drugs into PFC nanoparticles. Moreover, the rate of addition of safflower oil was maintained at nearly 5 mL/min for better coacervation[20].

The characteristics of the nanoparticle are summarized in Table 1. The findings suggest that particles smaller than 300 nm are well suited for an effective intravenous drug delivery system[21, 22]. This report reveals that DxP-NPs and DxA-NPs are similar in size (200−250 nm). Both are suitable candidates for SMC-targeted therapy because these particles can penetrate through microfissures into the vascular media. In the present study, the potential site-directed nanoparticles were incorporated with tissue factor antibody, which has high avid-

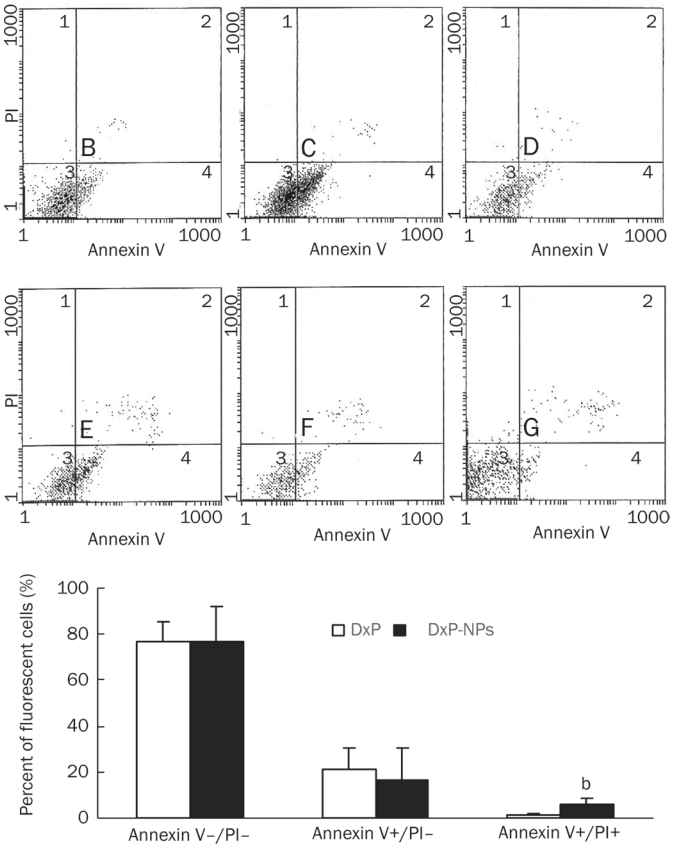

Figure 7. Apoptotic activity of DxP or TF-targeted DxP-NPs. The scatter plots (top) show that there was enhancement in apoptosis of SMCs treated with TF-targeted DxP-NPs (E, F, G) compared to that of free DxP (B, C, D). The percentage of the respective population is given in the quadrant. Quadrant 1, dead cells; Quadrant 2, late apoptotic cells; Quadrant 3, viable cells; Quadrant 4, early apoptotic cells. The bars (bottom) represent the percentage of fluorescent cells after exposure to DxP or TF-targeted DxP-NPs for 4 h. The values reported are means±SD of three separate experiments. $^{b}P<0.05$ (*vs* DxP-treated values for each experimental condition tested).

ity for smooth muscle cell membranes *in vivo*[23] and may be readily detected with diagnostic imaging modalities. Targeted nanoparticles bound to medial smooth muscle cells could also provide a unique vehicle to deliver antiproliferative chemotherapeutic agents, like those eluting off stents in the lumen, directly within the balloon-injured vascular wall.

Surface potentials play an important role in maintaining the stability of nanoparticles due to electrostatic repulsion[24]. The DxP-NPs exhibited a lower charge than either free NPs or DxA-NPs ($P<0.05$). The significant difference between DxP and DxA is that DxP is ionic and freely soluble in water. The effect of electrostatic repulsion is expected to decrease with increasing ionic strength, due to the decrease in the screening effect and diffusivity[25]. Since DxP is a relatively linear molecule with a charged hydrophilic group on one side and the hydrophobic group on the other, it is reasonable to expect DxP to be surface-active and form micelles. However, the decrease in diffusivity due to aggregation of DxP into micelle still needs to be further verified.

DxA-NPs have a relatively higher encapsulation efficiency (95.3%±1.3%) compared to DxP-NPs (66.4%±1.0%, $P<0.05$). PFC nanoparticles are distinctly different from other oil-based emulsions by virtue of the perfluorinated chains, which are extremely hydrophobic and lipophobic. Therefore, during microfluidization, a more hydrophobic form of the drug DxA (partition coefficient: log $P=2.91$) partitioned away from the water phase and the PFC core to reside in the hydrophobic lipid surfactant layer, which resulted in an increase of encapsulation efficiency within PFC NPs. To the contrary, the partition coefficient of DxP is very low, which caused a decrease in the drug content within the NPs due to drug migration toward the outer water phase. In addition, PFC nanoparticle emulsions are heterogeneous mixtures, formulated by at least one immiscible liquid intimately dispersed in another[11]. The incorporation of lipids could lead to crystal order disturbances on the lipid matrix of the PFC nanoparticles, thus leaving enough space to accommodate other molecules.

The release of DxA and DxP from PFC nanoparticles *in vitro* is depicted in Figure 2. The burst release of hydrophilic DxP from PFC nanoparticles is possibly due to the influence of the hydrophobic backbone and the lipid outlayer. The lower solubility of DxP in the lipid layer results in an increased amount of free DxP and decreased EE compared to the DxA-NPs. During the *in vitro* dissolution assay, surfactants act in an important role to maintain the stability of NPs in suspension[26]. When DxA is released from NPs, the surfactant attaches to the hydrophobic NP surface and prevents the drug from diffusing back into the solid core of the nanoparticles. We noticed that DxA exhibited a nearly linear release from PFC NPs during 7 d of administration, whereas there was about 17% DxP remaining within the NPs. Both of the NP-loaded drugs maintained release over one week.

The aim of this study was to develop SMC-targeted drug delivery nanoparticles loaded with dexamethasone as a drug model for anti-restenosis therapy. It is interesting to note that dexamethasone has been used in many *in vitro* and *in vivo* anti-proliferative studies[7, 27]. DxP is a water-soluble anti-inflammatory steroid more commonly used than DxA in the therapy of serious types of inflammatory diseases. In this study, the antiproliferative effect of free DxP and TF-targeted DxP-NPs on proliferating SMCs was evaluated *in vitro*. It was noted that the proliferation of SMCs was inhibited by DxP in a dose-dependent manner (Figure 4). However, other studies have found that the highly concentrated local delivery of an anti-restenotic agent, such as from a drug-eluting stent, not only inhibited neointima proliferation but also resulted in a loss of general vessel wall integrity. Since the therapeutic window of dexamethasone is very narrow[23], it was necessary to formulate an SMC-targeted drug delivery system that allows for release within this window.

PFC, which was used as a backbone of the nanoparticles, had no obvious cytotoxicity. Compared to free DxP, the TF-targeted DxP nanoparticles markedly decreased cell numbers

(P<0.05) and destroyed the structure of SMCs (Figure 5). In this study, free DxP demonstrated moderate inhibition of proliferation compared to TF-targeted DxP-NPs (Table 2). This could be explained by the differences obtained when analyzing the drugs in solution. Targeted drug delivery nanoparticles could bind, and the close apposition to the targeted cell membrane may permit enhanced lipid-lipid exchange with the lipid monolayer of the nanoparticle, which propels drugs dissolved in the outer lipid membrane of the nanoparticles into the targeted cells, enhancing the inhibition effect on SMCs. Cleek[28] *et al* also demonstrated that prolonged contact of the drug with SMCs could result in growth inhibition. Thus, a continuous exposure of cells to dexamethasone is probably necessary for sustained inhibition of proliferation.

SMC proliferation and migration from the tunica media to the intima are key mechanisms of intimal hyperplasia and atherosclerosis. SMC migration is a complex response to vascular injury that is mediated through various chemoattractants. In this report, the transwell migration assay showed that SMC migration was significantly inhibited by TF-targeted DxP-NPs compared to treatment with free DxP (P<0.05). TF-targeted DxP-NPs also result in more late stage apoptotic SMCs than free DxP (P<0.05). Isner[29] *et al* observed that apoptosis was most frequent in hypercellular tissue specimens typical of restenosis, which suggested a potential role in the maintenance of stable cell numbers in tissues with various degrees of proliferative activity. The TF-targeted DxP-NPs could stimulate more SMCs into late stage of apoptosis, which is usually an irreversible process of programmed cell death. This effect could ameliorate the reaction of intimal hyperplasia induced by percutaneous transluminal angioplasty, and provide a great opportunity for anti-restenosis therapy using a nanoparticle drug delivery system.

Conclusion

In this report, we demonstrate that DxP- and DxA-loaded PFC NPs exhibited better profile of encapsulation efficiency and sustained release *in vitro*. Compared to free drug, TF-targeted DxP-NPs manifested an enhanced effect on the inhibition of SMC proliferation and migration.

Acknowledgments

This work is supported by the Science and Technology Commission of Shanghai Municipality, China (0852nm05100). The authors wish to thank Professor Jennifer GAMBLE for critical review of the manuscript. We also thank the Central Research Institute of Shanghai Pharmaceutical (Group) Co for providing the high-pressure homogenizer.

Author contribution

Ji-wei ZHANG and Zhao-xiong ZHOU designed the study; Bai-gen ZHANG, Hao ZHANG and Xiao-zhong HUANG conducted the analysis; Ya-li HU and Li SUN contributed new analytical tools and reagents; Xiao-min WANG analyzed the data; Zhao-xiong ZHOU wrote the manuscript.

References

1 Schainfeld RM. Potential emerging therapeutic strategies to prevent restenosis in the peripheral vasculature. Catheter Cardiovasc Interv 2002; 56: 421–31.
2 Shah PB, Lilly CM. Interventional therapy for coronary artery disease. Am J Respir Crit Care Med 2002; 166: 791–6.
3 Costa MA, Simon DI. Molecular basis of restenosis and drug-eluting stents. Circulation 2005; 111: 2257–73.
4 Kolodgie FD, John M, Khurana C, Farb A, Wilson PS, *et al*. Sustained reduction of instent neointimal growth with the use of a novel systemic nanoparticle paclitaxel. Circulation 2002; 106: 1195–8.
5 Dibra A,Kastrati A, Mehilli J, Pache J,Schühlen H, *et al*. Paclitaxel-eluting or sirolimus-eluting stents to prevent restenosis in diabetic patients. N Engl J Med 2005; 353: 663–70.
6 Jaschke B, Michaelis C, Milz S, Vogeser M, Mund T, *et al*. Local statin therapy differentially interferes with smooth muscle and endothelial cell proliferation and reduces neointima on a drug-eluting stent platform. Cardiovasc Res 2005; 68: 483–92.
7 Patti G, Pasceri V, Carminati P, D'Ambrosio A, Carcagnì A, Di Sciascio G. Effect of dexamethasone-eluting stents on systemic inflammatory response in patients with unstable angina pectoris or recent myocardial infarction undergoing percutaneous coronary intervention. Am J Cardiol 2005; 95: 502–5.
8 Joner M, Finn AV, Farb A, Mont EK, Kolodgie FD, Ladich E, *et al*. Pathology of drug-eluting stents in humans: delayed healing and late thrombotic risk. J Am Coll Cardiol 2006; 48: 193–202.
9 Harald Vik-Mo, Rune W, Knut H. Coronary aneurysm after implantation of a paclitaxel-eluting stent. Scandinavian Cardiovasc J 2004; 38: 349–52.
10 Sarker DK. Engineering of nanoemulsions for drug delivery. Curr Drug Deliv 2: 297–310.
11 Lanza GM, Winter P, Caruthers S, Schmeider A, Crowder K, Morawski A, *et al*. Novel paramagnetic pontrast agents for molecular imaging and targeted drug delivery. Curr Pharm Biotechnol 2004; 5: 495–507.
12 Lanza GM, Yu X, Winter PM, Abendschein DR, Karukstis KK, Scott MJ, *et al*. Targeted antiproliferative drug delivery to vascular smooth muscle cells with a magnetic resonance imaging nanoparticle contrast agent: Implications for rational therapy of restenosis. Circulation 2002; 106: 2842–7.
13 Dong YC, Feng SS. Methoxy poly (ethylene glycol)-poly(lactide) (MPEG-PLA) nanoparticles for controlled delivery of anticancer drugs. Biomaterials 2004; 25: 2843–9.
14 Gallicchio M, Argyriou S, Ianches G, Filonzi EL, Zoellner H, Hamilton JA, *et al*. Stimulation of PAI-1 expression in endothelial cells by cultured vascular smooth muscle cells. Arterioscler Thromb Vasc Biol 1994; 14: 815–23.
15 Cordelier P, Esteve JP, Rivard N, Marletta M, Vaysse N, Susini C, *et al*. The activation of neuronal NO synthase is mediated by G-protein βγ subunit and the tyrosine phosphatase SHP-2. FASEB 1999: 132037–50.
16 Chaulet H, Desgranges C, Renault MA, Dupuch F, Ezan G, Peiretti F, *et al*. Extracellular nucleotides induce arterial smooth muscle cell migration via osteopontin. Circ Res 2001; 89: 772–8.
17 Mayr M, Li C, Zou Y, Huemer U, Hu Y, Xu Q. Biomechanical stress-induced apoptosis in vein grafts involves p38 mitogen-activated protein kinases. FASEB 2000; 14: 261–70.
18 Wickline SA, Lanza GM. Nanotechnology for molecular imaging and targeted therapy. Circulation 2003; 107: 1092–5.
19 Winter PM, Schmieder AH, Caruthers SD, Keene JL, Zhang H, Wickline SA, *et al*. Minute dosages of $\alpha_v\beta_3$-targeted fumagillin nanoparticles impair Vx-2 tumor angiogenesis and development in rabbits. FASEB

2008; 22: 2758–67.
20 Nihant N, Grandfiles C, Jerome R, Teyssie P. Microencapsulation by coacervation of poly (lactid-co-glycolide), IV: effect of the processing parameters on coacervation and encapsulation. J Control Release 1995; 35:117–25.
21 Song CX, Labhasetwar V, Cui XM, Underwood T, Levy RJ. Arterial uptake of biodegradable nanoparticles for intravascular local drug delivery: Results with an acute dog model. J Control Release 1998; 54: 201–11.
22 Guzman LA, Labhasetwar V, Song CX, Jang YS, Lincoff AM, Levy R, *et al*. Local intraluminal infusion of biodegradable polymeric nanoparticles. A novel approach for prolonged drug delivery after balloon angioplasty. Circulation 1996; 94: 1441–8.
23 Lanza GM, Abendschein DR, Hall CS, Marsh JN, Scott MJ, Scherrer DE, *et al*. Molecular imaging of stretch induced tissue factor expression in carotid arteries with intravascular ultrasound. Invest Radiol 2000; 35: 227–34.
24 Huang ZR, Hua SC, Yang YL, Fang JY. Development and evaluation of lipid nanoparticles for camptothecin deliver: a comparison of solid lipid nanoparticles, nanostructured lipid carriers, and lipid emulsion. Acta Pharmacol Sin 2008; 29: 1094–102.
25 Kima J, Chauhan A. Dexamethasone transport and ocular delivery from poly(hydroxyethyl methacrylate) gels. Int J Pharm 2008; 2: 205–22.
26 Kim Dong-Hwan, Martin DC. Sustained release of dexamethasone from hydrophilic matrices using PLGA nanoparticles for neural drug delivery. Biomaterial 2006; 27: 3031–7.
27 Zweersa LT, Engbersa HM, Grijpmaa DW, Feijen J. Release of antirestenosis drugs from poly(ethylene oxide)-poly(*dl*-lactic-co-glycolic acid) nanoparticles. J Control Release 2006; 114: 317–24.
28 Cleek RL, Rege AA, Denner LA, Eskin SG, Mikos AG. Inhibition of smooth muscle cell growth *in vitro* by an antisense oligodeoxynucleotide released from poly (*DL*-lactic-co-glycolic acid) microparticles. J Biomed Mater Res 1998; 35: 525–30.
29 Isner JM, Kearney M, Bortman S, Passeri J. Apoptosis in human atherosclerosis and restenosis. Circulation 1995; 91: 2703–11.